

DSAC-C: Constrained Maximum Entropy for Robust Discrete Soft-Actor Critic

Dexter Neo, Tsuhan Chen

School of Computing
National University of Singapore
e0534450@u.nus.edu, tsuhan@nus.edu.sg

Abstract

We present a novel extension to the family of Soft Actor-Critic (SAC) algorithms. We argue that based on the Maximum Entropy Principle, discrete SAC can be further improved via additional statistical constraints derived from a surrogate critic policy. Furthermore, our findings suggests that these constraints provide an added robustness against potential domain shifts, which are essential for safe deployment of reinforcement learning agents in the real-world. We provide theoretical analysis and show empirical results on low data regimes for both in-distribution and out-of-distribution variants of Atari 2600 games. Our code is available anonymously for review at: <https://anonymous.4open.science/r/MaxEnt-RL-ED5A>.

1 Introduction

Model-free deep reinforcement learning (RL) algorithms have received much success in a large number of challenging applications such as video games (Mnih et al. 2013; Silver et al. 2016) and robotic control tasks (Schulman et al. 2015; Gu et al. 2016). The usage of function-approximators such as neural networks in RL gives rise to promising potential in automating control and decision making tasks.

Unfortunately, current RL algorithms often make the closed-world assumption, i.e., that state-transitions follow a Markov Decision Process which is in-distribution (ID) with the training experience. This can cause RL agents to fail during deployment, since they do not have the ability to identify and preserve the learnt policy when it encounters out-of-distribution (OOD) states. These unexpected OOD states can lead to potentially dangerous situations. For example, a self-driving agent learned on a clean urban environment, may potentially fail catastrophically when deployed in a mountainous region. Furthermore, RL agents are often expensive to train (Obando-Ceron and Castro 2021) and we ideally want our agents to remain robust despite the potential unknown changes in environments.

Recent solutions to modern deep RL tasks can be broadly organized into three divisions of algorithms.

1. **Policy-gradient:** TRPO, (Schulman et al. 2015), PPO (Schulman et al. 2017). These require new samples to be collected in order to compute the gradients for policy

update. Which may lead to poor sample efficiency, with the number of gradient steps needed to learn an optimal policy tied to the task complexity.

2. **Value-based:** DQN (Mnih et al. 2013), Double DQN (Hasselt, Guez, and Silver 2015), C51 (Bellemare, Dabney, and Munos 2017), dueling networks (Wang et al. 2015) and Rainbow (Hessel et al. 2017). These aim to provide value estimates of a given state and are considered off-policy since the use of experience replay is involved. The combination of neural networks and off-policy learning can be problematic for stability and convergence (Maei et al. 2009). It is worth mentioning that Rainbow is a combination of the aforementioned value-based algorithms and prioritized experience replay (Schaul et al. 2015), multi-step bootstrap targets (Sutton and Barto 2018) and exploration with parameter noise (Fortunato et al. 2017).
3. **Actor-Critic:** These seek to combine both policy and value based methods A3C (Mnih et al. 2016), IMPALA (Espeholt et al. 2018), DDPG (Lillicrap et al. 2015), TD3 (Fujimoto, van Hoof, and Meger 2018) but can be brittle and sensitive to hyperparameter settings.

Although, these algorithms have enabled substantial improvements in solving deep RL tasks. The study of OOD RL tasks remains relatively unexplored with many previous works focusing on value-based methods. In contrast, we ask the question on how would soft actor-critic methods perform on OOD discrete tasks?

Originally proposed for continuous RL settings, SAC (Haarnoja et al. 2018a) was designed to tackle the many underlying issues of TD3 and DDPG. Based on the maximum entropy framework, the authors propose to append an additional entropy term to the objective function. The entropy term helps the agent naturally improve exploration and has achieved state-of-the-art performance on continuous RL benchmarks such as Mujoco (Todorov, Erez, and Tassa 2012). Although SAC’s remarkable performance on continuous action spaces has been largely successful, its discrete counterpart has not received much attention. Furthermore, many tasks involve discrete actions and require an alternate version of SAC.

The translation of SAC from continuous to discrete actions was first proposed by (Christodoulou 2019) where a di-

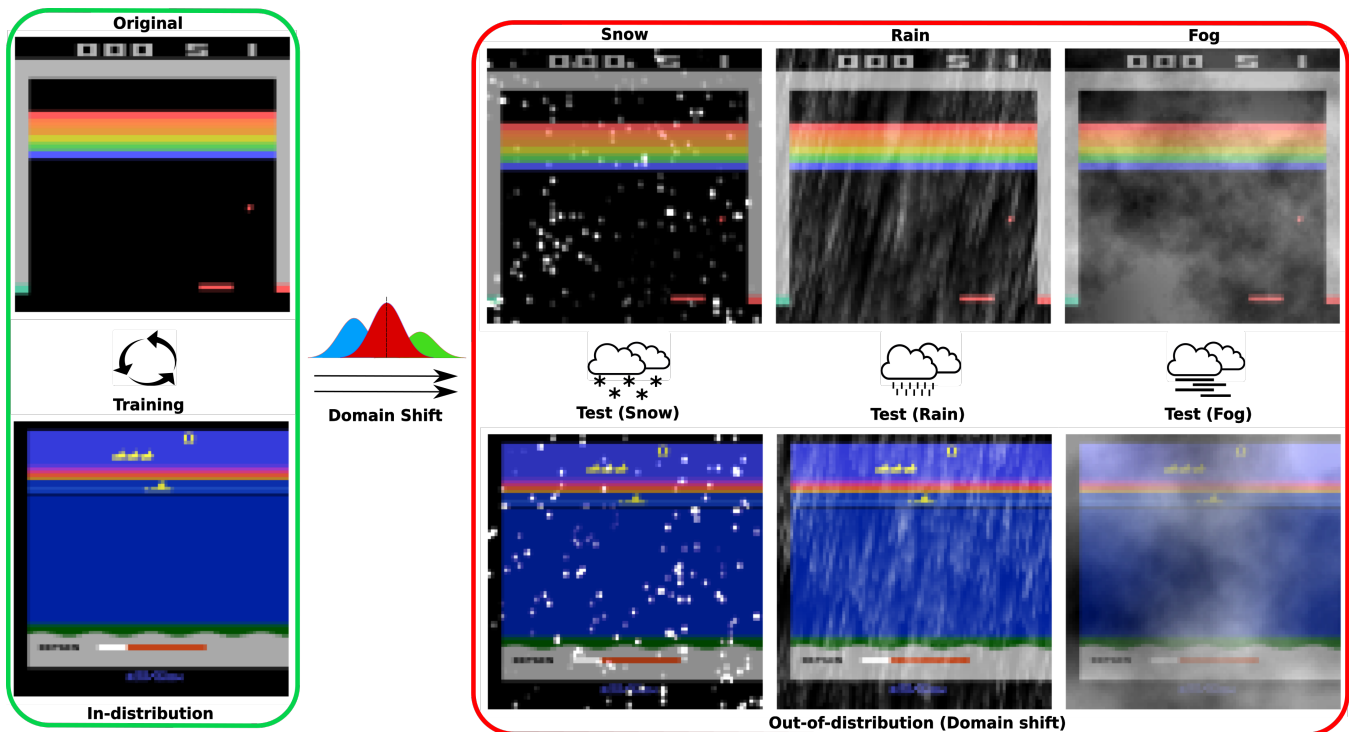


Figure 1: Screenshots of two Atari games, Breakout (top) and Seaquest (bottom). Agents are learned using in-distribution environments but evaluated on naturally occurring out-of-distributions shifts, emulating possible scenarios during deployment.

rect discretization of the action spaces is applied. Many authors believe that the maximum entropy SAC framework can benefit both continuous and discrete domains. However, empirical experiments from (Xu et al. 2021; Zhou et al. 2022) suggests that discrete SAC (DSAC) suffers from instability issues and underperforms on discrete benchmarks such as Atari ALE 2600 (Bellemare et al. 2012). Furthermore, there is still no general consensus within the community for a practical variant of discrete SAC.

Contrary to previous works, we revisit the classical idea of the Maximum Entropy framework (Jaynes 1957) and illustrate how additional constraints can be included for improving agent performance. We also further investigate the performance of DSAC on OOD states. We provide systematic comparisons on agent performance and behaviours on a suite of ID and makeshift OOD Atari environments. In Figure 1, we illustrate the problem setup for potential OOD states that agents could face during deployment. Such as "Snow", "Rain" or "Fog" which mimics the likely issues agents could face in the open-world, i.e., self-driving cars, patrol robots. Our contributions are summarized as follows:

1. **Constrained Maximum Entropy:** We revisit a theoretical link between the Principle of Maximum Entropy and DSAC, exploring how introducing constraints can help improve agent performance.
2. **Expected Value Targets:** We introduce a simple surrogate policy and expected value targets that are derived directly from the soft critic.
3. **DSAC-C Lagrangian:** We propose the mean and vari-

ance constraint forms of the discrete Soft Actor-Critic algorithm complete with automated Lagrange multiplier tuning for off-policy, model-free deep reinforcement learning.

4. **Evaluation on OOD Atari 2600 suite:** Our experiments show that our approach can be used to improve SAC on both ID and OOD discrete RL benchmarks.

2 Related Work

Discrete Soft-Actor Critic Vanilla discrete SAC (Christodoulou 2019) was first introduced by directly adapting the action domain from continuous to discrete. However, discrete SAC has been unsuccessful and many authors have hypothesized different reasons to its poor performance. For example, (Xu et al. 2021) proposed a scheduling method to improve DSAC’s target entropy and temperature tuning. While (Zhou et al. 2022) propose entropy penalty and average Q-clipping to stabilize the policy and Q-value under-estimation.

Offline OOD RL Previous works on OOD RL often look at value-based methods, where issues stem from the assignment of high Q-value estimates for OOD states (Sedlmeier et al. 2019). Strategies imposed aim to tackle the variances in Q-values such as model ensembles (Osband, Aslanides, and Cassirer 2018), placing lower bounds and constraining action selection (Kumar et al. 2019, 2020) during Q-learning. In this paper, we take a different approach by looking at SAC and its robustness towards distribution shifts of the state space during deployment.

Constrained Reinforcement Learning Apart from SAC, the entropy regularization term has been well studied in other RL fields. For example, apart from maximizing rewards other necessary conditions such as safety/limited resource compute have to be satisfied (Liu, Halev, and Liu 2021). While constraints can include many forms, the most common approaches include Lagrangian methods such as SAC Lagrangian (Ha et al. 2020), WCSAC (Yang et al. 2021), IPO (Liu, Ding, and Liu 2020) and PID-Lagrangian (Stooke, Achiam, and Abbeel 2020).

Maximum Entropy In supervised learning, the MaxEnt method has been found to provide additional benefits such as regularization and improving calibration (Pereyra et al. 2017; Mukhoti et al. 2020). For reinforcement learning, the MaxEnt method has provided benefits such as robustness against perturbations in environments and reward signal (Eysenbach and Levine 2022) and soft policy gradients (Shi, Song, and Wu 2019).

3 Preliminaries

3.1 Notation

We provide an overview of the notations and definitions used for infinite-horizon Markov decision processes (MDP). For a given standard MDP defined by the tuple $(\mathcal{S}, \mathcal{A}, \mathcal{T}, r, \gamma)$, where the state-action space are represented by \mathcal{S}, \mathcal{A} , with $\mathcal{T} : \mathcal{S} \times \mathcal{S} \times \mathcal{A} \rightarrow [0, \infty)$ given as the transition probability from the current state $s_t \in \mathcal{S}$ to the next state $s_{t+1} \in \mathcal{S}$ for action $a_t \in \mathcal{A}$ at timestep t . For each transition, the environment emits an immediate reward signal $r(s_t, a_t)$ and $\gamma \in [0, 1]$ is the discount factor. For deep actor-critic algorithms, the actor network ϕ learns a stochastic policy $\pi_\phi(a_t|s_t)$ for a given state from the gradients provided by the Q-value estimates $Q_\theta(s_t, a_t)$ of the critic network θ . In essence, the actor behaves as an approximate sampler, which attempts to estimate the true posterior of the given MDP, whilst the critic attempts to provide the best values estimates for a given state-action pair.

3.2 Principle of Maximum Entropy

The Principle of Maximum Entropy¹ (MaxEnt) is a probability distribution with the maximum entropy subject to the expected characteristic constraints. Formally, the general form of the MaxEnt method is given by the following objective:

$$\begin{aligned} \max \mathcal{H}(p(y_n|x_n)) &= \mathbb{E}[-\log p(y_n|x_n)] \\ \text{s.t. } \mathbb{E}[f_i(y)] &\leq c_i \text{ for all constraints } f_i(y) \end{aligned} \quad (1)$$

where $p(y_n|x_n)$ are the supervised learning estimates of the posterior distribution for the n th sample in the minibatch and $f_i(y)$ is an arbitrary characteristic function of the possible class outcomes y_n given input x_n for each respective constraint c_i . The characteristic functions are probability weighted in the form of $\mathbb{E}_{y \sim p}[f_i(y)] = \sum_y p(y)f_i(y)$. Without these constraints, the corresponding distribution which fulfills the maximum entropy for discrete tasks is simply the uniform distribution.

¹ We refer readers to (Jaynes 1957) for the fundamentals behind the Principle of Maximum Entropy.

3.3 Soft-Actor Critic

For standard RL problems, the goal is to maximize the expected sum of rewards $\mathbb{E}_{(s_t, a_t)}[\gamma^t r(s_t, a_t)]$. For maximum entropy reinforcement learning tasks, the goal is to maximize the expected sum of rewards along with an additional entropy term. The augmented maximum entropy objective favours stochastic policies (Haarnoja et al. 2018a) and the general entropy-regularized objective function (Ziebart 2010) for maximum entropy RL is given by the following expectation:

$$\pi^* = \arg \max_{\pi} \sum_{t=0}^T \mathbb{E}_{(s_t, a_t)}[\gamma^t r(s_t, a_t) + \alpha \mathcal{H}(\pi(\cdot|s_t))] \quad (2)$$

where π^* denotes the optimal policy for the MDP and the entropy function for the policy is given as $\mathcal{H} = -\alpha \sum_{\mathcal{A}} \pi(\cdot|s_t) \log \pi(\cdot|s_t)$. The corresponding temperature hyperparameter α is used to control the strength of the entropy term. In order to optimize the learning objective in Equation (2), actor-critic algorithms can be modified to incorporate the Maximum Entropy Method and alternates between 1.) Policy evaluation; where the critic is updated according to a soft Bellman target and 2.) Policy improvement; where the actor is updated via minimizing the Kullback-Leibler (KL) divergence between the $\pi_\phi(a_t|s_t)$ and $Q_\theta(s_t, a_t)$. 3.) Automatic tuning of α ; where the temperature parameter is updated according to constraints placed.

Soft Bellman Update: For a given policy and state, the probability weighted soft value estimates for the SAC algorithm are:

$$V(s_t) = \mathbb{E}_{a_t \sim \pi}[\min_{i=1,2} Q_{\theta_i}(s_{t+1}, a_{t+1}) - \alpha \log(\pi_\phi(s_t))] \quad (3)$$

where $V(s_t)$ is evaluated from two critics θ_i by taking the min value of the double-critic trick. The critics are learned by computing the tabular targets using the Bellman update equation:

$$\begin{aligned} J_Q(\theta) &= \mathbb{E}_{(s_t, a_t) \sim D}[(Q_\theta(s_t, a_t) \\ &- (r(s_t, a_t) + \gamma \mathbb{E}_{s_{t+1} \sim \mathcal{T}} V(s_{t+1})))^2] \end{aligned} \quad (4)$$

with the critic update given by the method of *temporal differences* (Sutton and Barto 2018) sampled from the experiences collected and stored in the replay buffer D .

Policy Update: For the policy improvement step, the actor is updated in the direction that maximizes the rewards as learned by the critic. The policy improvement step can be given by the KL divergence:

$$\pi_{new} = \arg \min D_{KL}[\pi(\cdot|s_t) || \frac{\exp(\frac{1}{\alpha} Q_{old}^\pi(s_t))}{Z_{old}^\pi(s_t)}] \quad (5)$$

For continuous action tasks, the policy is modified using the reparameterization trick, such that the actor ϕ outputs a mean and standard deviation which are used to define a Gaussian policy. In contrast, for discrete tasks the actor is required to output an action probability distribution $\pi_\theta(a_t|s_t)$ instead of a probability density. Therefore, there is no need for the reparameterization trick or the policy to be in the

form of a mean and variance for the action distribution. We can instead directly estimate the action distribution by applying the softmax function such that $\sum_A \pi_\phi(a_t|s_t) = 1$. The parameters of the actor are learned by minimizing the approximated form of the expected KL-divergence with the temperature parameter α :

$$J_\pi(\phi) = \mathbb{E}_{s_t \sim D} [\alpha \log(\pi_\phi(s_t)) - Q_\theta(s_t, a_t)] \quad (6)$$

Automatic Entropy Adjustment: The temperature parameter α regulates the actor’s entropy during exploration. Since the magnitude of rewards can not only vary across different games, the Q-estimates from the critics tend to become larger as the policy improves during training. Enforcing the entropy term to a fixed temperature can be regarded as a poor solution since the actor should be free to explore more across uncertain states and behave deterministic in states which are certain. (Haarnoja et al. 2018b) proposed that the following can be regarded as a Lagrangian optimization problem

$$\begin{aligned} \max \mathbb{E} &= \left[\sum_{t=0}^T r(s_t, a_t) \right] \\ \text{s.t. } &\mathbb{E}_{s_t, a_t \sim \pi_\phi} [-\log \pi_t(a_t|s_t)] \geq \mathcal{H}_U, \forall t \end{aligned} \quad (7)$$

where the sum of rewards is maximized subject to the entropy constraint, with the minimum target expected entropy \mathcal{H}_U as the entropy of a uniform policy across all discrete actions. By setting the following objective with a loose upper limit on the target entropy, α can be obtained by minimizing:

$$J(\alpha) = \mathbb{E}_{(a|s) \sim \pi} [\alpha(-\log(\pi_\phi(a_t|s_t))) - \mathcal{H}_U] \quad (8)$$

3.4 Stabilizing Discrete Soft-Actor Critic

Previous studies have shown that vanilla DSAC is not immune to problems such as policy instability and Q-value underestimation. For example, the temperature parameter α is directly tied to the agent’s ability to explore and a poor initialization of the target entropy can hurt the automated value-entropy tuning and overall performance (Wang and Ni 2020; Xu et al. 2021). (Zhou et al. 2022) have proposed countermeasures such as introducing an entropy-penalty term and double average clipped Q-learning. In our work, we found the double average Q-learning trick to be useful in mitigating state value underestimation. Specifically, for the learning of the critic, the soft value estimates become:

$$V(s_t) = \mathbb{E}_{a_t \sim \pi} [\bar{Q}_{\theta_i}(s_{t+1}, a_{t+1}) - \alpha \log(\pi_\phi(s_t))] \quad (9)$$

where the min operator in Equation (3) is replaced by the average operator $\bar{Q}_{\theta_i}(s_{t+1}, a_{t+1})$ in the double-critic trick.

4 DSAC-C: Constrained Discrete Soft-Actor Critic

Following Section 3.2, the MaxEnt RL objective only considers the entropy term, without additional characteristic expectation constraints. In the following section, we propose the addition of the following constraints to the SAC objective function, with the target expected value constraints estimated from a surrogate critic policy. We further describe in detail the different components of our method as follows:

4.1 Surrogate Critic Policy

Following the SAC objective, it can be shown that for the maximum entropy RL, the greedy soft policy is simply a softmax over its Q values scaled by the temperature parameter α . Since as $\alpha \rightarrow 0$, the softmax operator simply tends to the max operator. We propose to introduce a surrogate policy π_θ derived directly from the Q-estimates as a mirror of the actor’s policy. We highlight that this is a separate surrogate policy from the critic and it is not to be confused with the actor’s policy π_ϕ . This surrogate critic policy serves as a supplementary form of guidance to the actor during training.

$$\pi_\theta(a_t|s_t) = \frac{e^{Q_\theta(s_t, a_t)/\alpha}}{\sum e^{Q_\theta(s_t, a_t)/\alpha}} \quad (10)$$

Proof. See Appendix A.1

4.2 Mean Constrained Soft-Actor Critic

Recall that the MaxEnt method in Section 3.2, allows for constraints to be placed to the maximum entropy objective. Following this, we propose that the expected characteristic constraints to be computed from the critics and the arbitrary function to be chosen as the Q-value estimates. Using the surrogate critic policy, the expected mean value targets for state-action pair s_t, a_t can be computed from the critics batch wise as $\mu_\theta = \mathbb{E}_{Q_\theta} [Q_\theta(s_t, a_t)]$. Therefore, the computed constraints can be added to Equation (6) with the newly proposed update for the mean constrained soft actor given by the following objective function:

$$\begin{aligned} J_\pi(\phi) &= \mathbb{E}_{s_t \sim D} [\alpha \log(\pi_\phi(a_t|s_t)) - Q_\theta(s_t, a_t)] \\ &+ \lambda_1 \underbrace{(\mathbb{E}_{Q_\theta} [Q_\theta(s_t, a_t)] - \mu_\theta)}_{\text{Mean constraint}} \end{aligned} \quad (11)$$

where the predicted probabilities of the actor and Q-values are used to compute its expected mean given as $\mathbb{E}_{Q_\theta} [Q_\theta(s_t, a_t)]$ which is minimized against the critic’s mean. λ_1 is the respective Lagrange multiplier for the mean constraint which can be computed numerically e.g. using Newton Raphson method for each given state sample per minibatch. Consequently, using the objective function in Equation (11), the new policy for the mean constrained actor is given as:

$$\pi_\phi^\mu(a_t|s_t) = \frac{e^{(Q_\theta(s_t, a_t) - \lambda_1 Q_\theta(s_t, a_t))/\alpha}}{\sum e^{(Q_\theta(s_t, a_t) - \lambda_1 Q_\theta(s_t, a_t))/\alpha}} \quad (12)$$

Proof. See Appendix A.2

4.3 Variance Constrained Soft-Actor Critic

Following the steps proposed in the expected mean constraint, the expected variance target can be computed from the critics in a similar way as $\sigma_\theta^2 = \mathbb{E}_{Q_\theta} [(Q_\theta(s_t, a_t) - \mu)^2]$. Using this definition, we can reuse the expected mean targets computed earlier, using the handy relationship $\sigma_\theta^2 = \mathbb{E}_{Q_\theta} [Q_\theta(s_t, a_t)^2] - \mathbb{E}_{Q_\theta} [Q_\theta(s_t, a_t)]^2$. Finally, the new objective function for the variance constrained soft actor is

Algorithm 1: The DSAC-C Algorithm

Data: Initialize memory replay buffer D ;

```
1: Initialize network parameters  $\theta_1, \theta_2, \phi$ 
2: for each iteration do
3:   for each environment timestep do
4:      $a_t \sim \pi_\phi(a_t|s_t)$  // Sample action following actor's policy
5:      $s_{t+1} \sim p(s_{t+1}|s_t, a_t)$  // Sample transition from the environment
6:      $D \leftarrow D \cup \{(s_t, a_t, r(s_t, a_t), s_{t+1})\}$  // Store transition into memory buffer
7:
8:   for each gradient update step do
9:      $\theta_i \leftarrow \theta_i - \beta_Q \hat{\Delta}_{\theta_i} J(\theta_i)$  // Update the critic's parameters
10:     $\phi \leftarrow \phi - \beta_\pi \hat{\Delta}_\phi J_\pi(\Phi)$  // Update the actor's parameters
11:     $\lambda_i \leftarrow \lambda_i + \Delta \lambda_i$  // Solve  $\lambda_i$  numerically using NewtonRaphson()
12:     $\alpha \leftarrow \alpha - \beta_\pi \hat{\Delta}_\alpha J_\alpha(\alpha)$  // Adjust temperature
13:     $\bar{Q}_i \leftarrow \tau Q_i + (1 - \tau) \bar{Q}_i$  // Update target critics parameters
14:
15: return  $\theta_1, \theta_2, \phi$ 
16: Function NewtonRaphson():
17:    $\delta = 1e-15$ 
18:   while  $g(\lambda) > \delta$  do
19:      $\lambda_{n+1} = \lambda_n - \frac{g(\lambda)}{g'(\lambda)}$  // Update Lagrange multipliers  $\lambda_i$ 
20:   return  $\lambda_i$ 
```

given as:

$$J_\pi(\phi) = \mathbb{E}_{s_t \sim D} [\alpha \log(\pi_\phi(s_t)) - Q_\theta(s_t, a_t) + \lambda_2 \underbrace{(\mathbb{E}_{Q_\theta} [(Q_\theta(s_t, a_t) - \mu_\phi)^2] - \sigma_\theta^2)}_{\text{Variance constraint}}] \quad (13)$$

Using this form, λ_2 is the corresponding Lagrange multiplier for the variance constraint, with the new policy for the variance constraint actor given as:

$$\pi_\phi^{\sigma^2}(a_t|s_t) = \frac{e^{(Q_\theta(s_t, a_t) - \lambda_2(Q_\theta(s_t, a_t) - \mu)^2)/\alpha}}{\sum e^{(Q_\theta(s_t, a_t) - \lambda_2(Q_\theta(s_t, a_t) - \mu)^2)/\alpha}} \quad (14)$$

Proof. See Appendix A.3

We highlight that our proposed methods are not equivalent to naively minimizing the cross-entropy between the actor's policy and surrogate critic's policy. Since the KL-divergence between the actor and critic is already considered in the original SAC objective, the additional constraints serve as an additional form of guidance from the critic during training. Combining all of the above proposed changes, we summarize our method in Algorithm 1 and show the respective mathematical derivations in the Appendix.

4.4 Taming of the Q

Q-value estimates tend to become larger as the agent becomes better at solving tasks. This can be problematic for the newly proposed policies, since computing the expectation involves taking the exponent of large Q-values. This would cause problems such as overflow and policy instability. To alleviate these issues, we propose the following

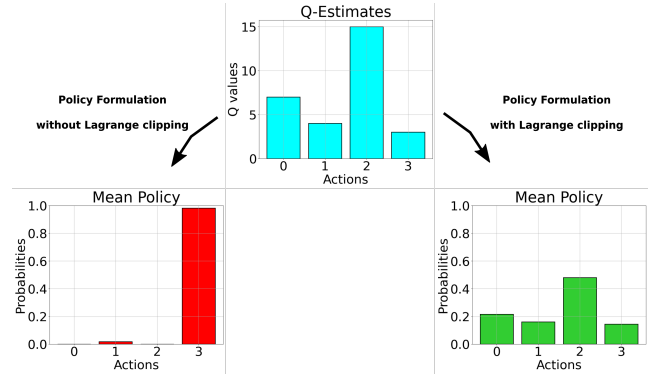


Figure 2: With Lagrange multiplier clipping, the constrained agent's policy is stable and aligned to the Q-values (green). Without clipping, the policy/argmax is lost (red).

workarounds to better manage these policies and the taming of large Q-values.

Lagrange Multiplier Clip: During the numerical finding of λ_i , these estimates can sometimes become too large or negative, causing a drastic change/flipping of policies. In Figure 2 we show an example of the failure case of the mean policy when λ_i is too large, with the change in the argmax of the greedy policy. Therefore, we propose to clip $\lambda_i \in [0-1]$, which bounds the constrained policy within small positive values. Specifically, if $\lambda_i = 0$ the original SAC policy in Equation (10) is obtained and the maximum penalty for the constraints are applied when $\lambda_i = 1$.

Stable Softmax Trick: To avoid overflow with large Q-

Environment	Alien	Amidar	Asterix	BattleZone	BeamRider	Breakout	CrazyClimber	Freeway	MsPacman	Seaquest	
ID	DSAC	292.33 ±88	16.33 ±17	1113.33 ±846	3333.33 ±1761	1821.70 ±543	34.60 ±13	408.00 ±575	14.40 ±10	357.67 ±43	50.50 ±20
	DSAC-M	288.33 ±44	14.57 ±12	1136.67 ±325	3033.33 ±1724	1454.40 ±335	70.70 ±65	1156.67 ±1530	21.50 ±0	379.00 ±65	172.77 ±194
	DSAC-V	315.00 ±126	2.33 ±2	923.33 ±123	3666.67 ±2330	2022.20 ±913	32.00 ±5	883.40 ±627	21.70 ±0	434.67 ±133	10.23 ±14
Snow	DSAC	104.33 ±28	3.23 ±2	350.00 ±181	3000.30 ±804	744.37 ±423	2.07 ±1	273.37 ±111	18.27 ±4	290.67 ±58	14.67 ±19
	DSAC-M	145.00 ±37	17.17 ±11	348.33 ±191	1067.97 ±330	384.93 ±215	2.37 ±0	50.00 ±36	21.37 ±1	269.00 ±139	124.50 ±46
	DSAC-V	175.00 ±65	4.43 ±4	350.00 ±175	2067.27 ±591	261.33 ±71	1.57 ±1	170.03 ±64	21.37 ±1	299.00 ±98	12.50 ±12
Rain	DSAC	241.67 ±12	5.67 ±6	595.00 ±482	4033.60 ±684	801.60 ±204	3.10 ±1	63.33 ±669	14.60 ±10	326.33 ±25	10.03 ±5
	DSAC-M	213.67 ±31	16.77 ±11	981.67 ±651	2233.83 ±1880	531.57 ±267	1.97 ±1	66.87 ±94	21.73 ±0	294.33 ±33	59.43 ±84
	DSAC-V	181.33 ±33	2.47 ±2	638.33 ±500	3667.03 ±1562	407.33 ±151	3.37 ±1	257.03 ±31	21.73 ±0	326.33 ±111	19.50 ±16
Fog	DSAC	164.00 ±15	1.33 ±0	296.67 ±182	867.37 ±619	476.53 ±244	2.93 ±1	46.67 ±66	14.43 ±10	195.00 ±54	11.33 ±16
	DSAC-M	144.33 ±7	7.33 ±3	311.67 ±165	2100.13 ±1675	621.07 ±103	2.73 ±1	30.00 ±10	21.57 ±0	182.00 ±60	71.97 ±72
	DSAC-V	122.67 ±16	1.57 ±0	293.33 ±181	3033.53 ±837	262.00 ±243	2.33 ±1	36.67 ±52	21.57 ±0	258.67 ±45	17.33 ±10
Overall	DSAC	DSAC-M	DSAC-M	DSAC	DSAC	DSAC-M	DSAC-V	DSAC-V	DSAC-V	DSAC-M	

Table 1: Raw return scores at 500,000 steps for each method benchmarked on Atari games across three random seeds. The best mean scores are in bold with \pm indicating 1 standard deviation. 1 training step equates to 4 consecutive stacked frames.

values, we can apply the stable softmax trick. This involves the subtraction of a constant (usually the maximum element) in the Q-values before raising the exponent. As an example, for Equation (10) the surrogate critic policy becomes $\frac{e^{Q_\theta(s_t, a_t) - \max(Q_\theta(s_t, a_t)) / \alpha}}{\sum e^{Q_\theta(s_t, a_t) - \max(Q_\theta(s_t, a_t)) / \alpha}}$. This trick ensures that the resulting exponent is mathematically equivalent to the original policy and does not affect gradient computation. We apply this trick for all Equations (10,12,14). For underflow, the resultant computation is simply regarded as zero.

5 Experiments and Results

In this section, we demonstrate the overall performance gains from the proposed constrained variants of DSAC on both ID and augmented OOD Atari. We further discuss the effects of these constraints on the policy’s entropy and expected value errors.

5.1 Experimental Setup

We benchmark our proposed algorithm against agents trained with vanilla D-SAC (Christodoulou 2019) Non ten different games from the Atari 2600 arcade learning environment (Bellemare et al. 2012). We begin each game with up to 30 no-op actions, so as to allow the agent a random starting position as per (Mnih et al. 2013). For our evaluation we follow the protocols of the respective author and test the deterministic policy of the agent after every 500,000 steps (2M frames) for 10 episodes with a cap of 5mins or 18000 frames across three different random seeds. We conduct our experiments on a NVIDIA RTX A5000 with Intel Xeon Silver 4310 CPU.

For our experiments we use CleanRL (Huang et al. 2022), with the additional details such as hyper-parameters used included in the Appendix. We use the imgaug (Jung et al. 2020) library to create the OOD shifted form of Atari, the augmentations are only applied during test time and not during training. We highlight that other forms of image augmentations (i.e. Gaussian Noise, Contrast, Saturation) can be used to evaluate agents, however we chose "Snow", "Rain" and "Fog" to simulate the more likely shifts from the real-world environment. Our algorithm does not require any supplementary data or tedious hyperparameter tuning (our Lagrange multipliers are computed on the fly during training).

5.2 ID Atari Evaluation

We compare both proposed mean and variance constraint forms against the baseline unconstrained form of DSAC. We show the learning curves for each environment along with the standard deviation across seeds indicated by shaded confidence bounds in Figure 3. From our experiments, we find that using constraints improves agent learning on nine out of the ten ID environments evaluated.

When comparing between the two forms of constraints, we find that the variance constraint form is able to consistently deliver better overall performance across five out of the eight games. While the mean constraint is able to obtain the highest scores in solving environments such as "Breakout" and "CrazyClimber", by about 104% and 183% increase in performance respectively. On environments where constraints did not improve ID performance, we observe a drop of about 10% for "Amidar".

5.3 OOD Atari Evaluation

Apart from evaluating our agent on ID Atari, we further demonstrate the performance gains of additional constraints on the makeshift OOD form of Atari. In general we observe improvements in seven out of the ten environments for each of the three domain shifts respectively. Due to the stochastic nature of reinforcement learning the improvements for each domain varies with each environment.

For example, in the "Snow" and "Rain" domain shifts constraints do not improve the "BattleZone" and "BeamRider" environments, however constrained DSAC performs better in the "Snow" domain. Coincidentally for each domain shift, we can observe that constraints help to improve OOD test performance in a total of seven out of ten environments. For the final overall performance, we equally consider the scores of each agent by summing their ID and OOD scores in the last row of Table 1. We find that with constraints, we are able to improve the general performance of DSAC in seven out of ten games. With the best performance from DSAC-M which improves four out of the seven environments.

5.4 Actor Entropy and Expected Value errors

We further examine the effects of the added constraints, by plotting the expected mean and variance errors along with

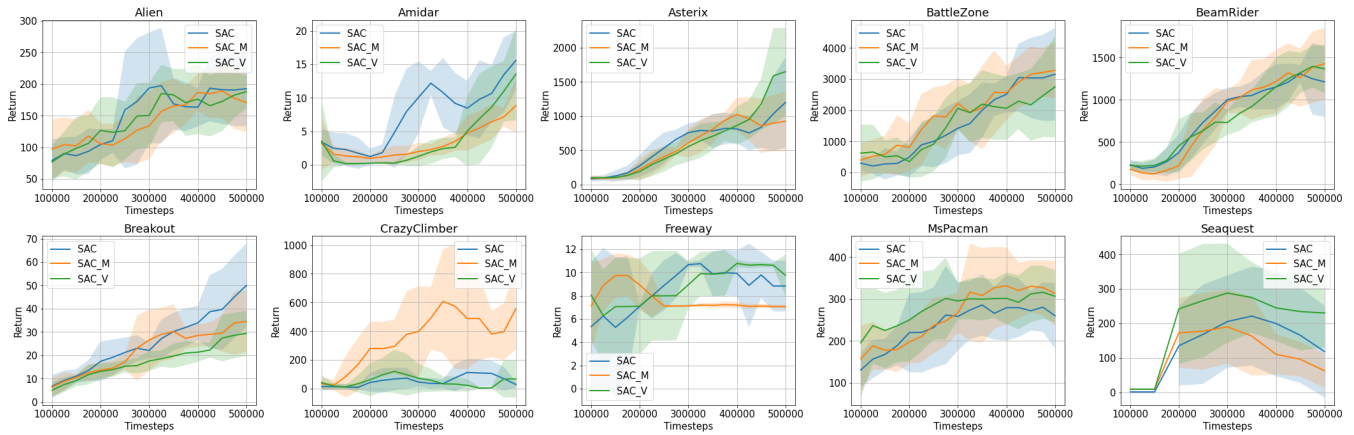


Figure 3: The learning curves on ten different Atari benchmarks, showing how additional constraints can be used to improve the overall performance of the SAC algorithm. Plots are smoothed for readability by a moving average of factor 10.

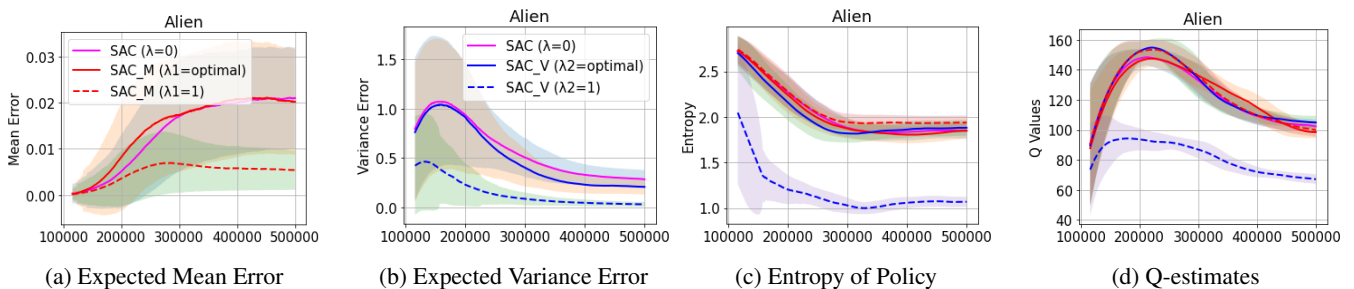


Figure 4: Additional constraints between the actor and critic’s expected values affects the policy’s entropy and Q-estimates during training.

the policy’s entropy and Q-estimates in Figure 4. Specifically, we measure the expected errors by taking the L1 difference between the actor and critic’s expected mean and variance values. We also plot the mean (red) and variance (blue) forms when the Lagrange multipliers are set to 1 (dotted) versus using the optimal (bold) Lagrange multipliers obtained numerically. For these plots, the temperature parameter α is fixed to 1.

Our findings suggests that the inclusion of constraints leads to lower expected value errors between the actor and critic. In both Figure 4a and Figure 4b, we can see that if the Lagrange multipliers are naively set to 1, lower value errors for both forms can be achieved. However, this can negatively cause the variance form to exhibit lower Q-value estimates and entropy. In contrast, when we use a numerical solver to obtain the optimal Lagrange multipliers we found training to be stable. With Q-estimates and entropy values bounded to similar performance of the unconstrained form.

6 Limitations and Future Work

Constraint Selection Similar to related works, we hypothesize that it is possible to further improve the constraint form of DSAC, with the inclusion of other forms of constraints. For example, apart from maximizing the reward function, additional constraints could be in the form of maximizing

safety in discrete domains/games.

Additional Training and Evaluation We positioned this paper for low-data regimes, however we believe that our proposed approach is able to obtain better and more consistent results with longer training times and extra evaluation across different seeds and games. Indeed, the current status-quo for proposing new reinforcement learning algorithms have been exacerbated to disclude newcomers without adequate computational resources.

7 Conclusion

We revisited a classical idea from the Principle of Maximum Entropy and proposed a novel addition to the SAC family using constraints derived from the critic. Our method includes modifications made to the actor’s objective function along with value function estimation and automated solving of the Lagrange multipliers for the constraints. We also show theoretical support for the new policy objectives and propose practical strategies to stabilize our method. Next, we benchmarked the overall performance gains against discrete SAC on both ID and OOD Atari. Finally, we discussed the different effects of the constraints on the expected value errors, actor’s entropy and Q-value estimates. However we fundamentally believe our approach is novel with encouraging experimental results.

References

- Bellemare, M. G.; Dabney, W.; and Munos, R. 2017. A Distributional Perspective on Reinforcement Learning. In *International Conference on Machine Learning*.
- Bellemare, M. G.; Naddaf, Y.; Veness, J.; and Bowling, M. 2012. The Arcade Learning Environment: An Evaluation Platform for General Agents (Extended Abstract). In *International Joint Conference on Artificial Intelligence*.
- Christodoulou, P. 2019. Soft Actor-Critic for Discrete Action Settings. *ArXiv*, abs/1910.07207.
- Espeholt, L.; Soyer, H.; Munos, R.; Simonyan, K.; Mnih, V.; Ward, T.; Doron, Y.; Firoiu, V.; Harley, T.; Dunning, I.; Legg, S.; and Kavukcuoglu, K. 2018. IMPALA: Scalable Distributed Deep-RL with Importance Weighted Actor-Learner Architectures. *ArXiv*, abs/1802.01561.
- Eysenbach, B.; and Levine, S. 2022. Maximum Entropy RL (Provably) Solves Some Robust RL Problems. In *International Conference on Learning Representations*.
- Fortunato, M.; Azar, M. G.; Piot, B.; Menick, J.; Osband, I.; Graves, A.; Mnih, V.; Munos, R.; Hassabis, D.; Pietquin, O.; Blundell, C.; and Legg, S. 2017. Noisy Networks for Exploration. *ArXiv*, abs/1706.10295.
- Fujimoto, S.; van Hoof, H.; and Meger, D. 2018. Addressing Function Approximation Error in Actor-Critic Methods. *ArXiv*, abs/1802.09477.
- Gu, S. S.; Holly, E.; Lillicrap, T. P.; and Levine, S. 2016. Deep reinforcement learning for robotic manipulation with asynchronous off-policy updates. *2017 IEEE International Conference on Robotics and Automation (ICRA)*, 3389–3396.
- Ha, S.; Xu, P.; Tan, Z.; Levine, S.; and Tan, J. 2020. Learning to Walk in the Real World with Minimal Human Effort. In *Conference on Robot Learning*.
- Haarnoja, T.; Zhou, A.; Abbeel, P.; and Levine, S. 2018a. Soft Actor-Critic: Off-Policy Maximum Entropy Deep Reinforcement Learning with a Stochastic Actor. In *ICML*.
- Haarnoja, T.; Zhou, A.; Hartikainen, K.; Tucker, G.; Ha, S.; Tan, J.; Kumar, V.; Zhu, H.; Gupta, A.; Abbeel, P.; and Levine, S. 2018b. Soft Actor-Critic Algorithms and Applications. *ArXiv*, abs/1812.05905.
- Hasselt, H. V.; Guez, A.; and Silver, D. 2015. Deep Reinforcement Learning with Double Q-Learning. In *AAAI Conference on Artificial Intelligence*.
- Hessel, M.; Modayil, J.; Hasselt, H. V.; Schaul, T.; Ostrovski, G.; Dabney, W.; Horgan, D.; Piot, B.; Azar, M. G.; and Silver, D. 2017. Rainbow: Combining Improvements in Deep Reinforcement Learning. In *AAAI Conference on Artificial Intelligence*.
- Huang, S.; Dossa, R. F. J.; Ye, C.; Braga, J.; Chakraborty, D.; Mehta, K.; and Araújo, J. G. 2022. CleanRL: High-quality Single-file Implementations of Deep Reinforcement Learning Algorithms. *Journal of Machine Learning Research*, 23(274): 1–18.
- Jaynes, E. T. 1957. Information Theory and Statistical Mechanics. *Physical Review*, 106: 620–630.
- Jung, A. B.; Wada, K.; Crall, J.; Tanaka, S.; Graving, J.; Reinders, C.; Yadav, S.; Banerjee, J.; Vecsei, G.; Kraft, A.; Rui, Z.; Borovec, J.; Vallentin, C.; Zhydenko, S.; Pfeiffer, K.; Cook, B.; Fernández, I.; De Rainville, F.-M.; Weng, C.-H.; Ayala-Acevedo, A.; Meudec, R.; Laporte, M.; et al. 2020. imgaug. <https://github.com/aleju/imgaug>. Online; accessed 01-Feb-2020.
- Kumar, A.; Fu, J.; Soh, M.; Tucker, G.; and Levine, S. 2019. Stabilizing Off-Policy Q-Learning via Bootstrapping Error Reduction. In Wallach, H.; Larochelle, H.; Beygelzimer, A.; d’Alché-Buc, F.; Fox, E.; and Garnett, R., eds., *Advances in Neural Information Processing Systems*, volume 32. Curran Associates, Inc.
- Kumar, A.; Zhou, A.; Tucker, G.; and Levine, S. 2020. Conservative Q-Learning for Offline Reinforcement Learning. In Larochelle, H.; Ranzato, M.; Hadsell, R.; Balcan, M.; and Lin, H., eds., *Advances in Neural Information Processing Systems*, volume 33, 1179–1191. Curran Associates, Inc.
- Lillicrap, T. P.; Hunt, J. J.; Pritzel, A.; Heess, N. M. O.; Erez, T.; Tassa, Y.; Silver, D.; and Wierstra, D. 2015. Continuous control with deep reinforcement learning. *CoRR*, abs/1509.02971.
- Liu, Y.; Ding, J.; and Liu, X. 2020. IPO: Interior-Point Policy Optimization under Constraints. *Proceedings of the AAAI Conference on Artificial Intelligence*, 34(04): 4940–4947.
- Liu, Y.; Halev, A.; and Liu, X. 2021. Policy Learning with Constraints in Model-free Reinforcement Learning: A Survey. In *International Joint Conference on Artificial Intelligence*.
- Maei, H. R.; Szepesvari, C.; Bhatnagar, S.; Precup, D.; Silver, D.; and Sutton, R. S. 2009. Convergent Temporal-Difference Learning with Arbitrary Smooth Function Approximation. In *NIPS*.
- Mnih, V.; Badia, A. P.; Mirza, M.; Graves, A.; Lillicrap, T. P.; Harley, T.; Silver, D.; and Kavukcuoglu, K. 2016. Asynchronous Methods for Deep Reinforcement Learning. In *International Conference on Machine Learning*.
- Mnih, V.; Kavukcuoglu, K.; Silver, D.; Graves, A.; Antonoglou, I.; Wierstra, D.; and Riedmiller, M. 2013. Playing atari with deep reinforcement learning. *arXiv preprint arXiv:1312.5602*.
- Mukhoti, J.; Kulharia, V.; Sanyal, A.; Golodetz, S.; Torr, P. H.; and Dokania, P. K. 2020. Calibrating Deep Neural Networks using Focal Loss. *Advances in Neural Information Processing Systems*.
- Obando-Ceron, J. S.; and Castro, P. S. 2021. Revisiting Rainbow: Promoting more insightful and inclusive deep reinforcement learning research. In *Proceedings of the 38th International Conference on Machine Learning*, Proceedings of Machine Learning Research. PMLR.
- Osband, I.; Aslanides, J.; and Cassirer, A. 2018. Randomized Prior Functions for Deep Reinforcement Learning. In Bengio, S.; Wallach, H.; Larochelle, H.; Grauman, K.; Cesa-Bianchi, N.; and Garnett, R., eds., *Advances in Neural Information Processing Systems*, volume 31. Curran Associates, Inc.

Pereyra, G.; Tucker, G.; Chorowski, J.; Łukasz Kaiser; and Hinton, G. 2017. Regularizing Neural Networks by Penalizing Confident Output Distributions. *arXiv 1701.06548*.

Schaul, T.; Quan, J.; Antonoglou, I.; and Silver, D. 2015. Prioritized Experience Replay. *CoRR*, abs/1511.05952.

Schulman, J.; Levine, S.; Abbeel, P.; Jordan, M. I.; and Moritz, P. 2015. Trust Region Policy Optimization. *ArXiv*, abs/1502.05477.

Schulman, J.; Wolski, F.; Dhariwal, P.; Radford, A.; and Klimov, O. 2017. Proximal Policy Optimization Algorithms. *ArXiv*, abs/1707.06347.

Sedlmeier, A.; Gabor, T.; Phan, T.; Belzner, L.; and Linnhoff-Popien, C. 2019. Uncertainty-Based Out-of-Distribution Detection in Deep Reinforcement Learning. *Digitale Welt*, 4: 74 – 78.

Shi, W.; Song, S.; and Wu, C. 2019. Soft Policy Gradient Method for Maximum Entropy Deep Reinforcement Learning. *ArXiv*, abs/1909.03198.

Silver, D.; Huang, A.; Maddison, C. J.; Guez, A.; Sifre, L.; van den Driessche, G.; Schrittwieser, J.; Antonoglou, I.; Panneershelvam, V.; Lanctot, M.; Dieleman, S.; Grewe, D.; Nham, J.; Kalchbrenner, N.; Sutskever, I.; Lillicrap, T. P.; Leach, M.; Kavukcuoglu, K.; Graepel, T.; and Hassabis, D. 2016. Mastering the game of Go with deep neural networks and tree search. *Nature*, 529: 484–489.

Stooke, A.; Achiam, J.; and Abbeel, P. 2020. Responsive Safety in Reinforcement Learning by PID Lagrangian Methods. In III, H. D.; and Singh, A., eds., *Proceedings of the 37th International Conference on Machine Learning*, volume 119 of *Proceedings of Machine Learning Research*, 9133–9143. PMLR.

Sutton, R. S.; and Barto, A. G. 2018. *Reinforcement Learning: An Introduction*. The MIT Press, second edition.

Todorov, E.; Erez, T.; and Tassa, Y. 2012. MuJoCo: A physics engine for model-based control. In *2012 IEEE/RSJ International Conference on Intelligent Robots and Systems*, 5026–5033. IEEE.

Wang, Y.; and Ni, T. 2020. Meta-sac: Auto-tune the entropy temperature of soft actor-critic via metagradient. *arXiv preprint arXiv:2007.01932*.

Wang, Z.; Schaul, T.; Hessel, M.; Hasselt, H. V.; Lanctot, M.; and de Freitas, N. 2015. Dueling Network Architectures for Deep Reinforcement Learning. In *International Conference on Machine Learning*.

Xu, Y.; Hu, D.; Liang, L.; McAleer, S.; Abbeel, P.; and Fox, R. 2021. Target Entropy Annealing for Discrete Soft Actor-Critic. *ArXiv*, abs/2112.02852.

Yang, Q.; Simão, T. D.; Tindemans, S. H.; and Spaan, M. T. J. 2021. WCSAC: Worst-Case Soft Actor Critic for Safety-Constrained Reinforcement Learning. In *Thirty-Fifth AAAI Conference on Artificial Intelligence*.

Zhou, H.; Lin, Z.; Li, J.; Ye, D.; Fu, Q.; and Yang, W. 2022. Revisiting Discrete Soft Actor-Critic. *ArXiv*, abs/2209.10081.

Ziebart, B. D. 2010. Modeling Purposeful Adaptive Behavior with the Principle of Maximum Causal Entropy. In *Doctoral thesis*.

A Appendix

In this section, we include the following proofs and mathematical derivations for discrete SAC. In Appendix A.1, we revisit the classical idea on how the actor’s policy can be directly derived from the Q value estimates, scaled by the temperature α . In the subsequent sections, Appendix A.2 and Appendix A.3, we look at how the actor’s objective can be modified with additional constraints derived from the critic. Following the additional constraints, we show how novel policies can be obtained for the mean and variance forms respectively, with the solutions provided for the Lagrange multipliers.

Previously mentioned in Algorithm 1, the Lagrange multipliers can be solved numerically, using a classical root-finder such as Newton’s method. We further show the proofs on how the Lagrange multipliers can be solved using the helper functions $g(\lambda)$ and its derivatives. Elegantly, the derivatives are found to be the negative variance (2nd momentum) for the mean constraint and negative kurtosis (4th momentum) for the variance constraint, which conveniently fit mathematically into the Newton’s method.

A.1 Discrete Soft-Actor Critic

$$J_\pi(\phi) = \sum \alpha \pi_\phi(s_t) \log \pi_\phi(s_t) - \pi_\phi(s_t) Q_\theta(s_t, a_t) + \lambda_0 (\sum \pi_\phi(a_t | s_t) - 1)$$

Expand the Lagrangian, take its derivative and set to zero

$$\frac{\partial J_\pi(\phi)}{\partial \pi_\phi(s_t)} = \alpha [\log \pi_\phi(s_t) + 1] - Q_\theta(s_t, a_t) + \lambda_0 = 0 \tag{1}$$

Subject to the following constraints

$$\sum \pi_\phi(a_t | s_t) = 1 \tag{2}$$

Rearrange Equation 1 and obtain general solution

$$\pi_\phi(s_t) = e^{-1 - \lambda_0 + Q_\theta(s_t, a_t) / \alpha} \tag{3}$$

Substitute general solution into first constraint

$$\pi_\phi(s_t) = \frac{1}{Z} \sum e^{Q_\theta(s_t, a_t) / \alpha} = 1 \tag{Let } Z = e^{1 + \lambda_0} \text{ and substitute } \underline{3} \text{ into } \underline{2}$$

Rearrange and obtain the soft actor’s policy

$$\pi_\phi(s_t) = \frac{e^{Q_\theta(s_t, a_t) / \alpha}}{\sum e^{Q_\theta(s_t, a_t) / \alpha}} \tag{4}$$

A.2 Mean Constraint form

$$J_\pi(\phi) = \sum \pi_\phi(s_t) \log \pi_\phi(s_t) - \pi_\phi(s_t) Q_\theta(s_t, a_t) + \lambda_0 (\sum \pi_\phi(a_t|s_t) - 1) + \lambda_1 (\sum \pi_\phi(a_t|s_t) Q_\theta(s_t, a_t) - \mu_\theta)$$

Expand the Lagrangian, take its derivative and set to zero

$$\frac{\partial J_\pi(\phi)}{\partial \pi_\phi(s_t)} = \log \pi_\phi(s_t) + 1 - Q_\theta(s_t, a_t) + \lambda_0 + \lambda_1 Q_\theta(s_t, a_t) = 0 \quad (1)$$

Subject to the following constraints

$$\sum \pi_\phi(a_t|s_t) = 1 \quad (2)$$

$$\sum \pi_\phi(a_t|s_t) Q_\theta(s_t, a_t) = \mu_\theta \quad (3)$$

Rearrange Equation 1 and obtain general solution

$$\pi_\phi(s_t) = e^{-1-\lambda_0+Q_\theta(s_t, a_t)-\lambda_1 Q_\theta(s_t, a_t)} \quad (4)$$

Substitute general solution into first constraint

$$\pi_\phi(s_t) = \frac{1}{Z} \sum e^{Q_\theta(s_t, a_t) - \lambda_1 Q_\theta(s_t, a_t)} = 1 \quad (\text{Let } Z = e^{1+\lambda_0} \text{ and substitute 4 into 2})$$

Rearrange and obtain the actor's policy

$$\pi_\phi(s_t) = \frac{e^{Q_\theta(s_t, a_t) - \lambda_1 Q_\theta(s_t, a_t)}}{\sum e^{Q_\theta(s_t, a_t) - \lambda_1 Q_\theta(s_t, a_t)}} \quad (5)$$

Satisfy second constraint

$$\sum \pi_\phi(s_t) Q_\theta(s_t, a_t) = \frac{\sum e^{Q_\theta(s_t, a_t) - \lambda_1 Q_\theta(s_t, a_t)} Q_\theta(s_t, a_t)}{\sum e^{Q_\theta(s_t, a_t) - \lambda_1 Q_\theta(s_t, a_t)}} = \mu_\theta \quad (\text{Substitute policy into 3})$$

Solve for λ_1 using Newton's method

$$g(\lambda_1) = \frac{\sum e^{Q_\theta(s_t, a_t) - \lambda_1 Q_\theta(s_t, a_t)} Q_\theta(s_t, a_t)}{\sum e^{Q_\theta(s_t, a_t) - \lambda_1 Q_\theta(s_t, a_t)}} - \mu_\theta$$

Take derivative of $g(\lambda_1)$ wrt λ_1 using the quotient rule

$$g'(\lambda_1) = \frac{-Q_\theta(s_t, a_t)^2 e^{Q_\theta(s_t, a_t) - \lambda_1 Q_\theta(s_t, a_t)} \sum e^{Q_\theta(s_t, a_t) - \lambda_1 Q_\theta(s_t, a_t)} + (Q_\theta(s_t, a_t)^2 e^{Q_\theta(s_t, a_t) - \lambda_1 Q_\theta(s_t, a_t)})^2}{(\sum e^{Q_\theta(s_t, a_t) - \lambda_1 Q_\theta(s_t, a_t)})^2}$$

Rearrange and obtain the final step for the derivative

$$g'(\lambda_1) = - \sum Q_\theta(s_t, a_t)^2 \frac{e^{Q_\theta(s_t, a_t) - \lambda_1 Q_\theta(s_t, a_t)}}{\sum e^{Q_\theta(s_t, a_t) - \lambda_1 Q_\theta(s_t, a_t)}} + \left(\sum Q_\theta(s_t, a_t) \frac{e^{Q_\theta(s_t, a_t) - \lambda_1 Q_\theta(s_t, a_t)}}{\sum e^{Q_\theta(s_t, a_t) - \lambda_1 Q_\theta(s_t, a_t)}} \right)^2$$

$$g'(\lambda_1) = -Var[Q_\theta] \quad (\text{Which gives the -ve Variance of the estimated Q-values})$$

A.3 Variance Constraint form

$$J_\pi(\phi) = \sum \pi_\phi(s_t) \log \pi_\phi(s_t) - \pi_\phi(s_t) Q_\theta(s_t, a_t) + \lambda_0 (\sum \pi_\phi(a_t|s_t) - 1) + \lambda_2 (\sum \pi_\phi(a_t|s_t) [Q_\theta(s_t, a_t) - \mu_\phi]^2 - \sigma_\theta^2)$$

Expand the Lagrangian, take its derivative and set to zero

$$\frac{\partial J_\pi(\phi)}{\partial \pi_\phi(s_t)} = \log \pi_\phi(s_t) + 1 - Q_\theta(s_t, a_t) + \lambda_0 + \lambda_2 [Q_\theta(s_t, a_t) - \mu_\phi]^2 = 0 \quad (1)$$

Subject to the following constraints

$$\sum \pi_\phi(a_t|s_t) = 1 \quad (2)$$

$$\sum \pi_\phi(a_t|s_t) [Q_\theta(s_t, a_t) - \mu_\phi]^2 = \sigma_\theta^2 \quad (3)$$

Rearrange Equation 1 and obtain general solution

$$\pi_\phi(s_t) = e^{-1-\lambda_0+Q_\theta(s_t, a_t)-\lambda_2[Q_\theta(s_t, a_t)-\mu_\phi]^2} \quad (4)$$

Substitute general solution into first constraint

$$\pi_\phi(s_t) = \frac{1}{Z} \sum e^{Q_\theta(s_t, a_t) - \lambda_2 [Q_\theta(s_t, a_t) - \mu_\phi]^2} = 1 \quad (\text{Let } Z = e^{1+\lambda_0} \text{ and substitute 4 into 2})$$

Rearrange and obtain the actor's policy

$$\pi_\phi(s_t) = \frac{e^{Q_\theta(s_t, a_t) - \lambda_2 [Q_\theta(s_t, a_t) - \mu_\phi]^2}}{\sum e^{Q_\theta(s_t, a_t) - \lambda_2 [Q_\theta(s_t, a_t) - \mu_\phi]^2}} \quad (5)$$

Satisfy second constraint

$$\sum \pi_\phi(s_t) [Q_\theta(s_t, a_t) - \mu_\phi]^2 = \frac{e^{Q_\theta(s_t, a_t) - \lambda_2 [Q_\theta(s_t, a_t) - \mu_\phi]^2}}{\sum e^{Q_\theta(s_t, a_t) - \lambda_2 [Q_\theta(s_t, a_t) - \mu_\phi]^2}} [Q_\theta(s_t, a_t) - \mu_\phi]^2 = \sigma_\theta^2 \quad (\text{Substitute policy into 3})$$

Solve for λ_2 using Newton's method

$$g(\lambda_2) = \frac{e^{Q_\theta(s_t, a_t) - \lambda_2 [Q_\theta(s_t, a_t) - \mu_\phi]^2}}{\sum e^{Q_\theta(s_t, a_t) - \lambda_2 [Q_\theta(s_t, a_t) - \mu_\phi]^2}} [Q_\theta(s_t, a_t) - \mu_\phi]^2 - \sigma_\theta^2$$

Take derivative of $g(\lambda_2)$ wrt λ_2 using the quotient rule

$$g'(\lambda_2) = \frac{-[Q_\theta - \mu_\phi]^4 e^{Q_\theta - \lambda_2 [Q_\theta - \mu_\phi]^2} \sum e^{Q_\theta - \lambda_2 [Q_\theta - \mu_\phi]^2} + ([Q_\theta - \mu_\phi]^2 e^{Q_\theta - \lambda_2 [Q_\theta - \mu_\phi]^2})^2}{(\sum e^{Q_\theta - \lambda_2 [Q_\theta - \mu_\phi]^2})^2}$$

Rearrange and obtain the final step for the derivative

$$g'(\lambda_2) = - \sum [Q_\theta - \mu_\phi]^4 \frac{e^{Q_\theta - \lambda_2 [Q_\theta - \mu_\phi]^2}}{\sum e^{Q_\theta - \lambda_2 [Q_\theta - \mu_\phi]^2}} + \left(\sum [Q_\theta - \mu_\phi]^2 \frac{e^{Q_\theta - \lambda_2 [Q_\theta - \mu_\phi]^2}}{\sum e^{Q_\theta - \lambda_2 [Q_\theta - \mu_\phi]^2}} \right)^2$$

$$g'(\lambda_2) = -K_{ur}[Q_\theta] \quad (\text{Which gives the -ve Kurtosis of the estimated Q-values})$$

B Hyperparameters

Hyperparameters	Values
learning rate	3e-4
optimizer	Adam
mini-batch size	64
discount γ	0.99
buffer size	10e5
hidden layers	2
hidden units per layer	512
activation function	ReLU
target smoothing coefficient τ	1.00
target entropy discount	0.98

Table 2: Hyperparameters used for Discrete SAC and constrained variants

Environment	Alien	Amidar	Asterix	BattleZone	BeamRider	Breakout	CrazyClimber	Freeway	MsPacman	Seaquest	
ID	DSAC	287.23 \pm 28	19.60 \pm 12	4737.06 \pm 1516	1729.33 \pm 260	1497.14 \pm 561	50.05 \pm 6	190.90 \pm 151	16.34 \pm 2	435.63 \pm 52	265.09 \pm 215
	DSAC-M	241.93 \pm 24	9.72 \pm 2	1137.46 \pm 690	3753.61 \pm 242	1040.48 \pm 327	47.12 \pm 4	255.16 \pm 123	18.49 \pm 2	478.33 \pm 23	279.56 \pm 250
	DSAC-V	279.00 \pm 38	16.16 \pm 7	1189.83 \pm 281	3340.42 \pm 409	1234.35 \pm 368	38.76 \pm 3	374.36 \pm 261	17.79 \pm 2	470.07 \pm 40	148.14 \pm 22
Snow	DSAC	142.73 \pm 18	5.22 \pm 2	410.00 \pm 141	1923.95 \pm 276	387.16 \pm 62	2.08 \pm 0	91.04 \pm 36	16.47 \pm 2	254.50 \pm 27	82.30 \pm 36
	DSAC-M	129.13 \pm 12	7.39 \pm 5	375.67 \pm 143	1583.73 \pm 529	340.05 \pm 103	2.16 \pm 0	212.43 \pm 207	18.00 \pm 3	322.90 \pm 28	66.18 \pm 42
	DSAC-V	132.23 \pm 12	5.21 \pm 2	344.83 \pm 110	2007.24 \pm 418	336.35 \pm 92	2.42 \pm 0	185.14 \pm 58	17.39 \pm 2	250.27 \pm 10	59.66 \pm 6
Rain	DSAC	166.77 \pm 24	3.60 \pm 2	560.17 \pm 192	2663.90 \pm 292	554.53 \pm 238	2.76 \pm 1	73.42 \pm 42	16.51 \pm 2	370.57 \pm 18	188.19 \pm 160
	DSAC-M	182.93 \pm 9	3.25 \pm 2	398.67 \pm 201	2120.52 \pm 83	253.07 \pm 52	2.42 \pm 0	57.34 \pm 20	18.56 \pm 2	413.43 \pm 33	188.20 \pm 150
	DSAC-V	188.40 \pm 28	4.98 \pm 3	414.00 \pm 165	2420.22 \pm 171	282.85 \pm 126	2.44 \pm 0	120.60 \pm 136	17.83 \pm 2	362.63 \pm 39	121.64 \pm 21
Fog	DSAC	181.17 \pm 20	4.84 \pm 2	386.17 \pm 124	2800.34 \pm 225	452.24 \pm 184	2.51 \pm 0	38.45 \pm 24	16.37 \pm 2	247.03 \pm 18	103.13 \pm 75
	DSAC-M	172.40 \pm 3	6.95 \pm 5	346.17 \pm 84	2236.95 \pm 612	232.95 \pm 51	2.43 \pm 0	24.00 \pm 16	18.49 \pm 2	335.13 \pm 68	95.78 \pm 39
	DSAC-V	186.37 \pm 8	5.30 \pm 4	317.50 \pm 94	2523.50 \pm 249	361.71 \pm 91	2.42 \pm 0	81.21 \pm 35	17.67 \pm 2	244.13 \pm 38	72.80 \pm 15
Overall	DSAC	DSAC-M	DSAC-M	DSAC	DSAC	DSAC-M	DSAC-V	DSAC-V	DSAC-V	DSAC-M	

Table 3: Raw return scores at 500,000 steps for each method benchmarked on Atari games across three random seeds. The best mean scores are in bold with \pm indicating 1 standard deviation. 1 training step equates to 4 consecutive stacked frames.

Environment	Alien	Amidar	Asterix	BattleZone	BeamRider	Breakout	CrazyClimber	Freeway	MsPacman	Seaquest	
ID	DSAC	287.23 \pm 28	19.60 \pm 12	1729.33 \pm 260	1497.14 \pm 561	4737.06 \pm 1516	50.05 \pm 6	190.90 \pm 151	16.34 \pm 2	435.63 \pm 52	265.09 \pm 215
	DSAC-M	342.00 \pm 35	11.75 \pm 5	1205.00 \pm 498	1848.63 \pm 73	3836.93 \pm 442	43.52 \pm 7	359.60 \pm 464	17.09 \pm 1	500.13 \pm 56	128.29 \pm 25
	DSAC-V	285.30 \pm 31	13.41 \pm 2	1357.00 \pm 155	1442.80 \pm 179	3903.67 \pm 328	43.67 \pm 10	112.90 \pm 90	20.21 \pm 1	465.83 \pm 74	38.65 \pm 9
Snow	DSAC	142.73 \pm 18	5.22 \pm 2	410.00 \pm 141	387.16 \pm 62	1923.95 \pm 276	2.08 \pm 0	91.04 \pm 36	16.47 \pm 2	254.50 \pm 27	82.30 \pm 36
	DSAC-M	139.13 \pm 9	7.87 \pm 5	309.83 \pm 127	323.66 \pm 63	1663.88 \pm 364	2.81 \pm 0	276.42 \pm 361	17.38 \pm 2	314.23 \pm 24	43.00 \pm 13
	DSAC-V	146.03 \pm 15	6.73 \pm 2	302.50 \pm 133	288.49 \pm 77	1893.75 \pm 502	2.27 \pm 0	65.85 \pm 29	20.25 \pm 1	271.00 \pm 22	31.74 \pm 2
Rain	DSAC	166.77 \pm 24	3.60 \pm 2	560.17 \pm 192	554.53 \pm 238	2663.90 \pm 292	2.76 \pm 1	73.42 \pm 42	16.51 \pm 2	370.57 \pm 18	188.19 \pm 160
	DSAC-M	197.80 \pm 16	7.38 \pm 4	353.00 \pm 161	463.89 \pm 116	2023.60 \pm 108	2.63 \pm 0	121.79 \pm 157	17.16 \pm 2	362.70 \pm 23	91.21 \pm 6
	DSAC-V	166.17 \pm 3	4.46 \pm 2	385.00 \pm 220	364.21 \pm 118	1997.05 \pm 287	2.82 \pm 0	74.80 \pm 36	20.31 \pm 1	356.10 \pm 24	28.41 \pm 11
Fog	DSAC	181.17 \pm 20	4.84 \pm 2	386.17 \pm 124	452.24 \pm 184	2800.34 \pm 225	2.51 \pm 0	38.45 \pm 24	16.37 \pm 2	247.03 \pm 18	103.13 \pm 75
	DSAC-M	188.67 \pm 20	5.93 \pm 4	309.83 \pm 176	373.84 \pm 63	2160.25 \pm 591	2.38 \pm 0	97.00 \pm 97	17.08 \pm 2	296.77 \pm 65	70.73 \pm 12
	DSAC-V	165.57 \pm 15	4.77 \pm 2	285.83 \pm 101	417.11 \pm 147	2626.87 \pm 352	2.50 \pm 0	80.06 \pm 27	20.24 \pm 1	236.80 \pm 24	27.90 \pm 13
Overall	DSAC	DSAC-M	DSAC-M	DSAC	DSAC	DSAC-M	DSAC-V	DSAC-V	DSAC-V	DSAC-M	

Table 4: Raw return scores at 500,000 steps for each method benchmarked on Atari games across three random seeds. The best mean scores are in bold with \pm indicating 1 standard deviation. 1 training step equates to 4 consecutive stacked frames.